Contents lists available at ScienceDirect

Applied Surface Science

Preparation of PbS and PbO nanopowders from new Pb(II)(saccharine) coordination polymers

Alireza Aslani [a,b,∗], Seyid Javad Musevi [c], Ertan Şahin [d], Veysel T. Yilmaz [e,∗]

[a] Nanobiotechnology Research Center, Baqiyatallah University Medical of Science, PO BOX 1994x81, Tehran, Iran
[b] Department of Chemistry, University of Lorestan, Lorestan-Khoramabad 68135-465, Iran
[c] Department of Chemistry, Shahid Beheshti Technical and Vocational University, Urmia, Iran
[d] Department of Chemistry, Faculty of Science, Ataturk University, Erzurum 25240, Turkey
[e] Department of Chemistry, Faculty of Arts and Sciences, Uludag University, 16059 Bursa, Turkey

ARTICLE INFO

ABSTRACT

Nanopowders and single crystal of new Pb(II) three-dimensional coordination polymer, $[Pb(H_2O)(\mu\text{-}OAc)(\mu\text{-}sac)]_n$ "PASAC" were synthesized by a sonochemical and branched tube methods (Yılmaz et al., Z. Anorg. Allg. Chem. 629 (2003) 172). The new nano-structures of Pb(II) coordination polymer were characterized by X-ray crystallography analysis, scanning electron microscopy (SEM), X-ray powder diffraction (XRD), surface analysis (BET), and IR spectroscopy. The crystal structure of these compounds consists of three-dimensional polymeric units. The thermal stability of compounds was studied by thermal gravimetric analysis (TGA) and differential thermal analyses (DTA). PbS and PbO nano-structures were obtained by calcinations of the nano-structures of this coordination polymer at 600 °C.

Introduction

Nanopowders are a class of materials with properties distinctively different from their bulk and molecular counterparts. They are used in a variety of different areas, such as electronic, magnetic and optoelectronic, biomedical, pharmaceutical, cosmetic, energy, environmental, catalytic, and materials applications. Because of the potential of this technology, there has been a worldwide increase in investment in nanotechnology research and development [1,2]. Although extensive effort has been done for the synthesis of metals, oxides, sulfides, and ceramic materials with nanoscale dimension, little attention has given to date on supramolecular compounds such as coordination polymers.

Saccharin, ($C_7H_5NO_3S$) alternatively named 1,2-benzisothiazoline-3-(2*H*)one 1,1-dioxide or *o*-sulphobenzimide, and its water soluble alkali and earth-alkali salts are currently the most widely used non-caloric artificial sweetener in the world [3]. The presence of several potential donor atoms such as the imino nitrogen, one carbonyl and two sulfonyl oxygen atoms makes the saccharinate anion (sac) very interesting and versatile polyfunctional ligand. Therefore, it readily interacts with different metal ions [4–10]. It was reported that sac usually coordinates to transition metal ions as a monodentate ligand through the N atom and also in some cases with the O (carbonyl) atom, behaving as an ambidentate ligand [11,12]. Sac also acts as a bidentate or bridging ligand through the N and O (carbonyl) or O (sulfonyl) atoms [13,14]. The studies were mainly focused on synthesis and characterization of sac complexes with transition metals. However, sac complexes of p-block metals received less attention [15,18–20].

On the other hand, metal–organic compounds have been studied widely as they represent an important interface between synthetic chemistry and materials science. The synthesis of metal–organic compounds is often guided by the quest to understand how molecules can be organized and how functions can be achieved, and their specific structures, properties, and reactivity's not found in mononuclear compounds [21–26] have led to a wide range of potential applications as molecular wires, electrical conductors, molecular magnets, in host guest chemistry and in catalysis. In contrast to inorganic materials, the specific syntheses of nano-structured metal–organic compounds, seem to be surprisingly sparse. There have been only very few reports into the syntheses and properties of nano-materials being made up of coordination polymers [13]. Equally the use of organometallic

* Corresponding authors at: Nanochemistry, Chemistry, Andimeshk Highway, Jundi Shapur University of Technology, Dezful 5451847536, Khuzestan, Iran. Tel.: +98 9141261366; fax: +98 916 116 116 5/+98 641 6260993.
E-mail addresses: a.aslani110@yahoo.com, nanochemistry@yahoo.com (A. Aslani), Erkin_musevi@hotmail.com (S.J. Musevi), Ertan@atauni.edu.tr (E. Şahin), vtyilmaz@uludag.edu.tr (V.T. Yilmaz).

compounds as precursors for the preparation of inorganic nano-materials has not yet been investigated thoroughly. Sonochemistry is the research area in which molecules undergo a chemical reaction due to the application of powerful ultrasound radiation (20 kHz–10 MHz). In the recent years many kinds of nano-materials have been prepared by this method [27–31].

PbO nano particles have many application such as usage in dye and glass industry (lead glasses), piezoelectric ceramics, super-capacitors and lead–acid batteries. Nanometer-sized particles of metal coordination polymers are fascinating to explore, since their unique properties are controlled by the large number of surface molecules, which experience an entirely different environment than those in a bulk crystal. Several studies have been reported about the synthesis of PbO and PbS nanopowders [32–35], but if we look them carefully, morphology of finally products are very different from each other. Therefore use of the different ligands in initial materials can be changed the finally morphology of PbO and PbS. On the other hand, the aim of this study is to demonstrate the role of the initial ligands in the structure of the finally nanoparticles. It shown, that the initial ligands play important role in morphology of finally products, so this work is new precursor for preparation to synthesis an interest and different morphologies of PbS and PbO nanopowders.

This study focused on the synthesis of single crystal and nanopowders of new coordination polymer from Pb(II) acetate and saccharine ligand $[Pb(H_2O)(\mu\text{-OAc})(\mu\text{-sac})]_n$ "PASAC" and preparation the PbO and PbS nanopowders from the thermal decomposition of the nanopowders of this coordination polymer at 600 °C at different morphologies reported in other studies.

Experimental

All reagents and solvents were commercially available and were used as received. A multiwave ultrasonic generator (Bandlin Sonopuls Gerate-Typ: UW 3200, Germany), equipped with a converter/transducer and titanium oscillator (horn), 12.5 mm in diameter, operating at 24 kHz with a maximum power output of 600 W, was used for the ultrasonic irradiation. The ultrasonic generator automatically adjusts the power level. IR spectra were recorded using Perkin-Elmer 597 and Nicolet 510P spectrophotometers. Melting points were measured on an electro thermal 9100 apparatus and are uncorrected. The DTA and TGA data were obtained using a PL-STA 1500 apparatus and platinum crucibles with a heating rate of 5 °C min^{-1} in a static atmosphere of nitrogen. X-ray powder diffraction (XRPD) measurements were performed using a Philips diffractometer manufactured by X'pert with monochromatized Cu K_α radiation. Simulated XRPD patterns were calculated using Mercury based on the single crystal data. Particle sizes of selected samples were estimated using the Sherrer method. For characterization with a Scanning Electron Microscope, samples were gold coated. The specific surface area of samples was determined using the Brunauer–Emmet–Teller (BET) method in a volumetric adsorption apparatus (ASAP 2010 M, Micrometritics Instrument Corp).

Crystallography

For the crystal structure determination, the single-crystal of the compound "PASAC" was used for data collection on a four-circle Rigaku R-AXIS RAPID-S diffractometer (equipped with a two-dimensional area IP detector). The graphite-monochromatized Mo K_α radiation ($\lambda = 0.71073$ Å) and oscillation scans technique with $\Delta\omega = 5°$ for one image were used for data collection. The lattice parameters were determined by the least-squares methods on the basis of all reflections with $F^2 > 2\sigma(F^2)$. Integration of the

Table 1
Crystallographic data for (PASAC).

| Empirical formula	$C_9H_9NO_6PbS$
M_r	466.44
T (K)	293
Radiation (Å)	0.71073
Crystal system	Triclinic
Space group	P^-1
Unit cell dimensions	2
a (Å)	7.1607(3)
b (Å)	7.8167(3)
c (Å)	12.5453(4)
Cell angle (°)	$\alpha = 87.6437(53)$, $\beta = 75.0871(46)$, $\gamma = 64.7036(35)$
V (Å^3)	611.57(5)
Z	2
D_c (g/cm^3)	2.533
(mm^{-1})	13.981
$F(0 0 0)$	432
Crystal size (mm)	$0.12 \times 0.13 \times 0.16$
Range (°)	2.9 and 26.4
Index range (h, k, l)	$h(-8,8), k(-9,9), l(-15,15)$
Reflections collected	12890
Independent reflections (R_{int})	0.078
Absorption correction	Multiscan
Goodness-of-fit on F^2	1.133
Final R indices [$I > 2(I)$]	0.034 and 0.074
wR indices (all data)	0.036 and 0.090
Largest diff. peak and hole (e.Å^{-3})	0.890 and −0.539

Structural data's for single crystal of $[Pb(H_2O)(\mu\text{-OAc})(\mu\text{-Sac})]_n$.

intensities, correction for Lorentz and polarization effects and cell refinement was performed using crystal clear (Rigaku/MSC Inc., 2005) [16] software. The structures were solved by direct methods using SHELXS-97 and refined by a full-matrix least-squares procedure using the program SHELXL-97 [17]. The final difference Fourier maps showed no peaks of chemical significance. Crystal data for $[Pb(H_2O)(\mu\text{-OAc})(\mu\text{-sac})]_n$, bond distances, bond and torsion angles are given in Tables 1 and 2, respectively.

To prepare the nano-particles of $[Pb(H_2O)(\mu\text{-OAc})(\mu\text{-sac})]_n$, 15 ml of 0.1 M solution of lead(II) acetate in MeOH was positioned in a high-density ultrasonic probe, operating at 60 kHz with a maximum power output of 800 W. Into this solution a 10 ml of 0.3 M solution of the ligands saccharine (0.2 M) was added dropwise. The obtained precipitates were filtered, washed with methanol and then dried in air. Product 1: $M_p > 150$ °C. IR bands: 117m, 160w, 185w, 701m, 968m, 1148w, 1250w, 1340vs, 1430v, 1536vs, 1615v, 2020vs and 3065w. To isolate single crystals of $[Pb(H_2O)(\mu\text{-OAc})(\mu\text{-sac})]_n$, 0.5 mmol of saccharine, 0.189 g and 0.5 mmol Pb(II) acetate, 0.189 g were placed in the main arm of a branched tube. Methanol was carefully added to fill both arms. The tube was sealed and the ligand-containing arm immersed in an oil bath at 60 °C while the other arm was kept at ambient temperature. After 5 days, colorless crystals deposited in the cooler arm were isolated, filtered off, washed with acetone and ether and air dried. Product: $M_p > 330$ °C. Found: IR bands: 115m, 162w, 188w, 711m, 972m, 1150w, 1255w, 1345vs, 1432v, 1537vs, 1617v, 2020vs and 3065w.

Results and discussion

Scheme 1 gives an overview of the methods used for the synthesis of $[Pb(H_2O)(\mu\text{-OAc})(\mu\text{-sac})]_n$, and their conversion to PbS and PbO by calcination. The coordination complexes were obtained by reaction of sac with Pb(II) acetate in methanol. Single crystalline material was obtained using a heat gradient applied to a solution of the reagents (branched tube method) [26], while nanopowders
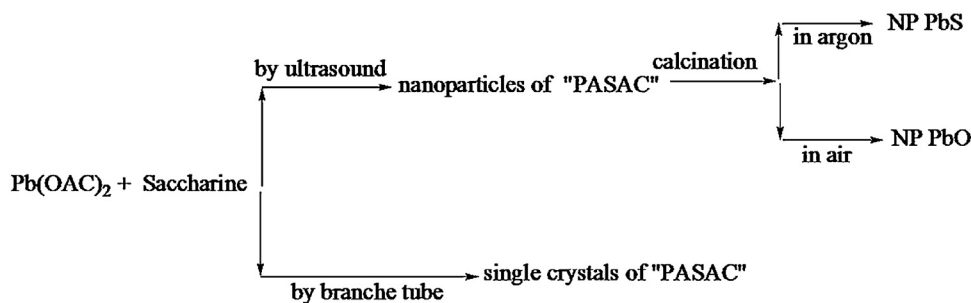
Scheme 1. Materials produced and synthetic methods.

of this coordination polymer were prepared by ultrasonication of the methanolic solution. The new Pb(II) coordination polymers, $[Pb(H_2O)(\mu\text{-}OAc)(\mu\text{-}sac)]_n$, are air-stable and soluble in DMSO. In the IR spectra, the band with strong intensity at 1617 cm^{-1} may be due to the $\nu(C\text{-}C)$ vibrations of the phenyl ring of sac. The absorption bands of the C–N–S moiety of sac are observed at 1345 and 972 cm^{-1}. The $\nu_{asym}(SO_2)$ and $\nu_{sym}(SO_2)$ modes of sac appear as very strong bands at 1255 cm^{-1} at 1150 cm^{-1}, respectively. The carbonyl stretching vibrations of the OAc moiety are clearly shown in the spectra of the Pb(II) complex (Table 1). The strong bands at around 1537 and 1432 cm^{-1} are attributed to the $\nu_{asym}(COO)$ and $\nu_{sym}(COO)$ modes of the carboxyl group of OAc, respectively. Many attempts were made previously to correlate the positions of the $\nu_{asym}(COO)$ and $\nu_{sym}(COO)$ modes or the frequency difference $\Delta\nu\,(\nu_{asym} - \nu_{sym})$ [23]. It was concluded that the frequency difference $\Delta\nu$ is usually in the range 162–188 cm^{-1} for ionic carboxylate groups, larger values being expected in the case of monodentate and lower values for bidentate coordination. The $\Delta\nu$ value of OAc in the Pb(II) complex is 115 cm^{-1} and in agreement with the expected bidentate and bridging coordination of OAc.

Table 2
Selected geometric parameters for the complex $[Pb(H_2O)(\mu\text{-}OAc)(\mu\text{-}Sac)]_n$ (Å and °).

Sample	Distance	Sample	Distance
Pb–N(1)	2.634(4)	Pb–O(4)	2.542(4)
Pb–O(5)	2.560(4)	Pb–O(6)	2.599(4)
S(1)–O(2)	1.425(4)	S(1)–O(3)	1.447(4)
S(1)–N(1)	1.610(4)	S(1)–C(7)	1.766(4)
O(4)–C(8)	1.238(5)	O(5)–C(8)	1.264(5)
C(2)–C(1)	1.498(4)	N(1)–C(1)	1.360(4)
C(4)–C(3)	1.397(4)	C(4)–C(5)	1.378(5)
C(8)–C(9)	1.495(5)	C(7)–C(6)	1.378(5)
C(6)–C(5)	1.368(5)	C(1)–O(1)	1.223(5)

Sample	Angle	Sample	Angle
O(2)–S(1)–O(3)	115.1(4)	O(2)–S(1)–N(1)	110.9(5)
O(2)–S(1)–C(7)	109.7(4)	O(3)–S(1)–N(1)	111.0(4)
O(3)–S(1)–C(7)	111.8(4)	N(1)–S(1)–C(7)	96.9(4)
C(7)–C(2)–C(1)	111.3(7)	C(7)–C(2)–C(3)	120.2(8)
S(1)–N(1)–C(1)	111.8(6)	O(4)–C(8)–O(5)	118.4(8)
O(4)–C(8)–C(9)	122.0(8)	O(5)–C(8)–C(9)	119.5(8)
S(1)–C(7)–C(2)	107.2(6)	S(1)–C(7)–C(6)	130.4(7)
C(2)–C(1)–N(1)	112.9(7)	C(2)–C(1)–O(1)	124.8(8)
N(1)–C(1)–O(1)	122.3(8)	–	–

Sample	Torsion	Sample	Torsion
O(2)–S(1)–N(1)–C(1)	−112.9	O(2)–S(1)–C(7)–C(2)	114.2
O(2)–S(1)–C(7)–C(6)	−67.7	O(3)–S(1)–N(1)–C(1)	117.8
O(3)–S(1)–C(7)–C(2)	−116.9	O(3)–S(1)–C(7)–C(6)	61.2
N(1)–S(1)–C(7)–C(2)	−0.9	N(1)–S(1)–C(7)–C(6)	177.2
C(7)–S(1)–N(1)–C(1)	1.3	C(1)–C(2)–C(7)–S(1)	0.4
C(7)–C(2)–C(1)–N(1)	0.5	C(1)–C(2)–C(7)–C(6)	−177.9
C(7)–C(2)–C(1)–O(1)	−180.0	C(3)–C(2)–C(7)–S(1)	−177.5

Fig. 1. shows the XRD patterns of typical samples of the complex prepared by the sonochemical process and the single crystal of "PASAC", and also the XRD patterns of simulated from single crystal X-ray data. Acceptable matches are observed for both compounds indicating the presence of only one crystalline phase in the samples prepared using the sonochemical process. The average size of the particles was found to be around 55 nm, estimated from the Scherer formula for the calculation of particle sizes from the broadening of the XRD peaks ($D = 0.8911/b(\cos\theta)$, where D is the average grain size, 0.8911 is the X-ray wavelength (0.15405 nm), and θ and b are the diffraction angle and full width at half maximum of an observed peak, respectively. The calculated value is in agreement with the value obtained from the SEM images shown in Fig. 2.

The structure of the complex produced by the branched tube method was determined by single crystal X-ray diffraction analysis. An ORTEP plot of the coordination polyhedron around the Pb(II) ion is shown in Fig. 3. Selected bond distances and angles are given in Table 2. The Pb(II) complex crystallizes in the triclinic crystal system with the space group of $P1^-$ with four units per cell. The complex exhibits a three-dimensional polymeric structure, in which the Pb(II) ion is seven-coordinate and possesses an PbNO$_6$ coordination environment by six oxygen atoms (one from the aqua ligand, one from the sac ligand and four from the OAc ligands) and the nitrogen atom of the sac ligand. The carboxylate moiety of the OAc ligand acts as both bidentate, and bridging group (totally tetradentate) in a μ-1, 3 mode, yielding one-dimensional infinite chains. These cha'ns are further bridged by the sac ligands into a three-dimensional framework as illustrated in Figs. 4 and 5. Within the chain the Pb(II) ions have a co-planar coordination making a *zigzag* arrangement and the intra-chain distance between two neighboring Pb(II) ions is *ca.* 4.268(2) Å. The Pb–N bond distances are significantly shorter than those found in other reported Pb(II) complexes [13]. The geometry of the nearest coordination environment of every lead atom in
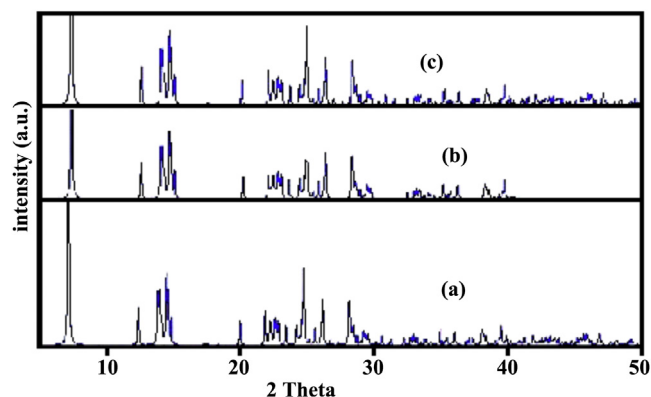

Fig. 1. The XRPD patterns 1: (a) nano-structured of (PASAC) prepared by the sonochemical method, (b) Single Crystal structure of (PASAC) prepared by branched tube method and (c) simulated from single crystal X-ray data of (PASAC).
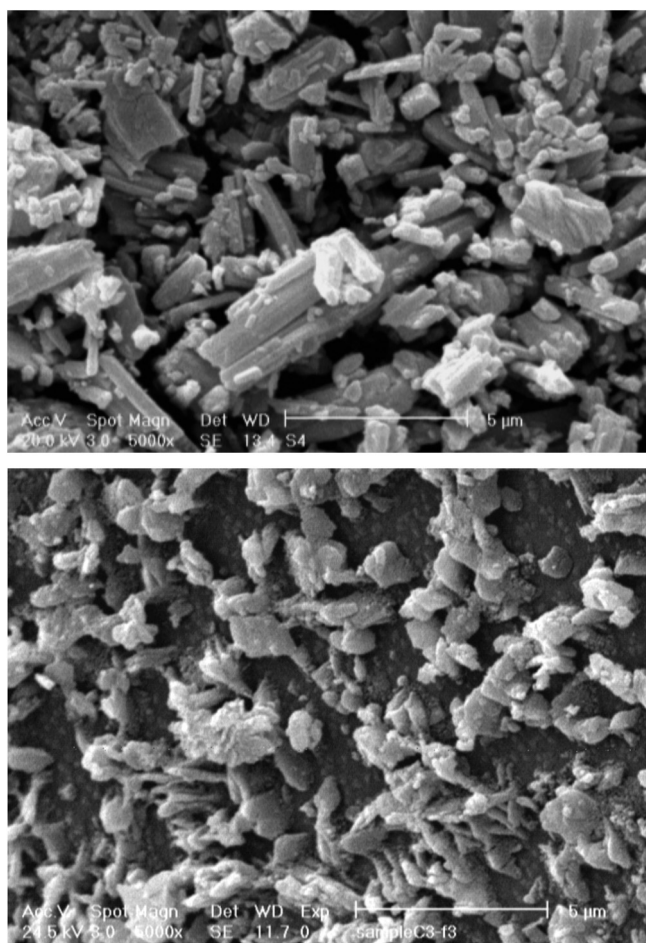
Fig. 2. SEM photograph of [Pb(H$_2$O)(μ-OAc)(μ-sac)]$_n$ nanoparticles.

Fig. 3. ORTEP View of the coordination polyhedron around lead(II) in [Pb(H$_2$O)(μ-OAc)(μ-sac)]$_n$ showing the atom numbering scheme. Ellipsoids represent thermal displacement parameters at the 40% probability level. Dashed lines indicates H-bonding geometry (symmetry code *i* = −*x*,−*y*,−*z*).
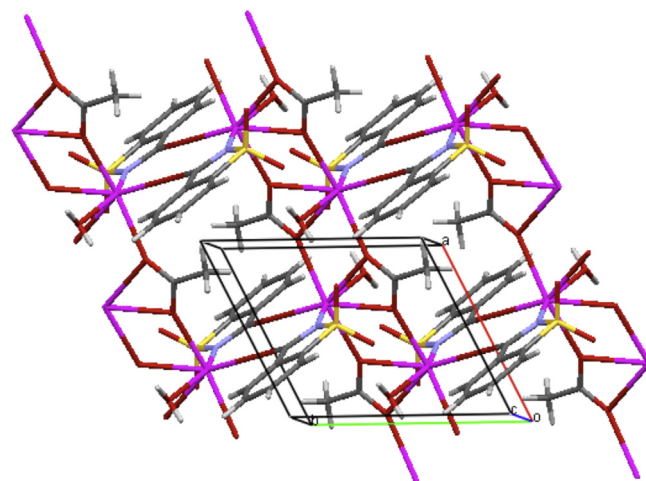

Fig. 4. Packing diagram of [Pb(H$_2$O)(μ-OAc)(μ-sac)]$_n$ Bridging of one-dimensinal polymeric chains by sac ligands forming a two-dimensional network.

compound is likely caused by an interplay of several factors: the geometrical constraints of the coordinated OAc and sac ligands and the influence of a stereo-chemically non-active lone pair of electrons. This results in a significant gap *trans* to the sac ligands and a hemidirected coordination around the lead atoms. This kind of the hemi directed geometry is in agreement with observations for other lead complexes with intermediate coordination numbers (6–8) in the presence of hard-donor ligands [36–41].
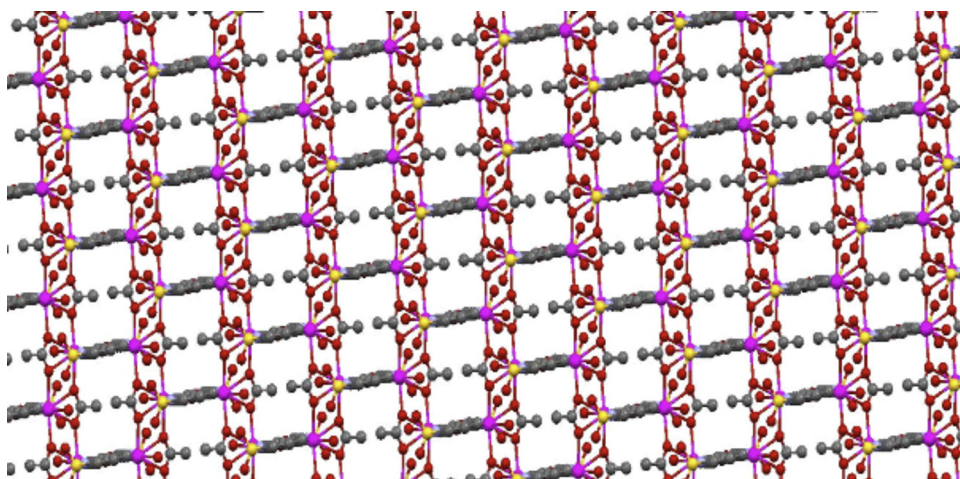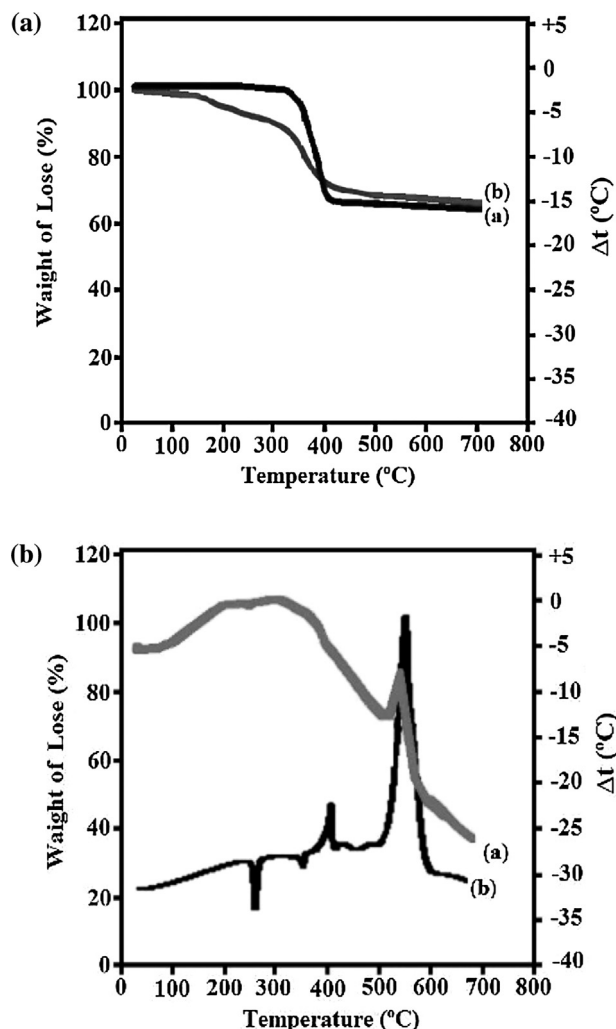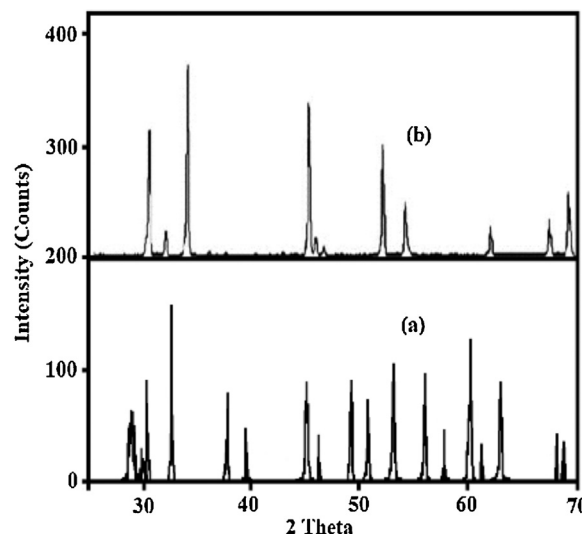

Fig. 5. Diagram of three-dimensional "PASAC" coordination polymer.

Fig. 6. (a) TGA curves of (PASAC): (a) nanopowders and (b) single crystals. (b) DTA curves of (PASAC): (a) nanopowders and (b) single crystals.

Fig. 7. XRPD patterns of PbO nanopowders (a) and PbS nanopowders (b) prepared by calcinations of compound (PASAC).

To examine the thermal stability of the nano-structured and single crystalline samples of compound, thermal gravimetric and differential thermal analyses (TGA and DTA) were carried out between 40 and 700 °C in a static atmosphere of nitrogen (Fig. 6). Single crystals of the compound is very stable and do not decompose up to a temperature of 363 °C. Decomposition of the compound occurs between 363 and 417 °C with a mass loss of 42.69% (calcd 39.50%). Mass loss calculations show that the final decomposition product is PbO (Fig. 7a and b). Nano-structure of compound is somewhat less stable and starts to gradually decompose at 110 °C. Decomposition ends at 500 °C and the total mass loss is 46.50% (calcinated 42.50%), indicating again PbO as the final decomposition product. Decomposition of compound nano-structure starts at about 110 °C earlier than its single crystals, probably due to reduction of the particle size of the coordination polymers to a few dozen nanometers results in lower thermal stability when compared to the single crystalline samples. For single crystals of compound the DTA curve displays a distinct endothermic effect at 280 °C and two exothermic effects at 410 and 570 °C. The TGA curves of the nanopowders have the same general appearance as those of their single crystalline counterparts and the endo and exothermic effects are retained for nanopowders. In agreement with the TGA results, some differences between the maximum intensities indicate the lower stability of the nanoparticles compared to those of their single crystals. Nano-structured PbO has

been generated by thermal decomposition of nanoparticle. The final product upon calcinations of the compound is, based on their XRD patterns (Fig. 7), in both cases cubic PbO and PbS. The XRD patterns of PbO and PbS nanopowders prepared by calcinations at 600 °C of basically identical. The obtained patterns match with the standard patterns of cubic PbO with $a = 4.0862$ Å and $Z = 2$. Figs. 8 and 9 show SEM images of PbO and PbS nanopowders, produced by calcinations of compound in air and argon.

The surface area analysis was carried out on "PASAC" at nano and bulk size by BET method. Assuming the particles possess solid, spherical shape with smooth surface and same size, the surface area can be related to the average equivalent particle size by the equation:

$$D_{BET} = \frac{6000}{(\rho S_w)(\text{in nm})}$$

where D_{BET} is the average diameter of a spherical particle; S_w represents the measured surface area of the powder in m^2/g; and ρ is the theoretical density in g/cm^3. Fig. 10 shows the BET plots of "PASAC" at nano and bulk size, the specific surface area of (PASAC)
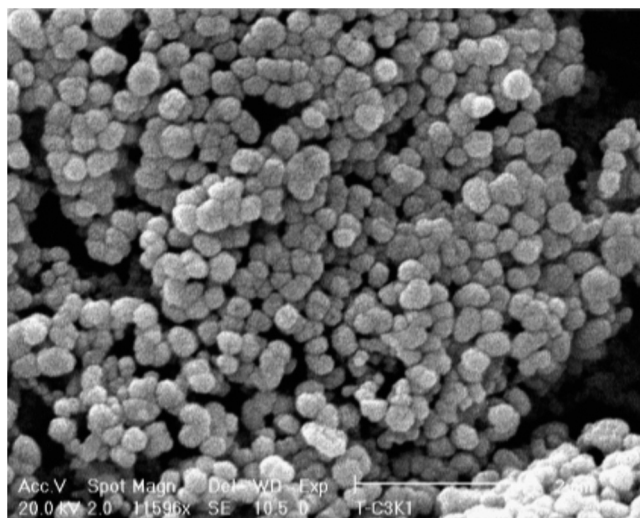
Fig. 8. SEM photograph of PbS nanopowders produced by calcination of compound (PASAC) under argon atmosphere.
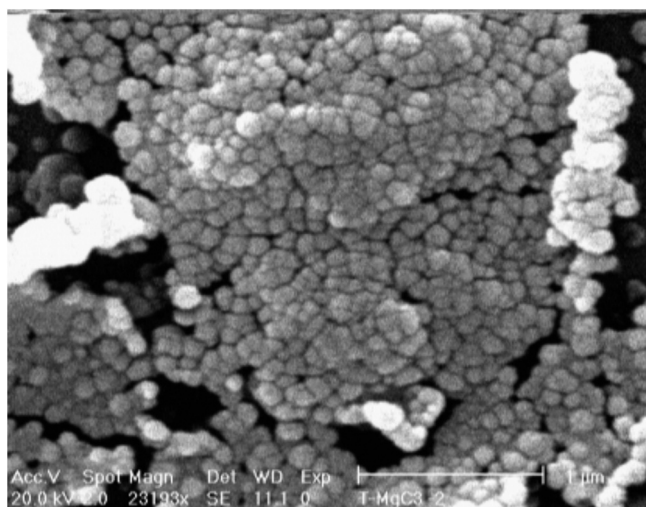
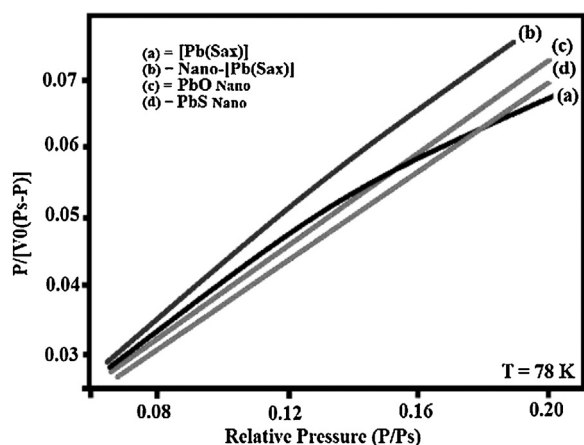**Fig. 9.** SEM photograph of PbO nanopowders produced by calcination of compound (PASAC) in air atmosphere.

Fig. 10. BET plots of (a) Bulk size of $[Pb(H_2O)(\mu\text{-}OAc)(\mu\text{-}sac)]_n$, (b) Nano size of $[Pb(H_2O)(\mu\text{-}OAc)(\mu\text{-}sac)]_n$, (c) PbO nanopowders and (d) PbS nanopowders.

at nano and bulk size, PbO and $PbBr_2$ calculated using the multi-point BET-equation are 74, 50, 27 and 31 m^2/g (layout for bulk size of $[Pb(H_2O)(\mu\text{-}OAc)(\mu\text{-}sac)]_n$, nano size of $[Pb(H_2O)(\mu\text{-}OAc)(\mu\text{-}sac)]_n$, PbO and PbS), and the calculated average equivalent particle size is 71, 41, 22 and 26 nm (layout for bulk size of $[Pb(H_2O)(\mu\text{-}OAc)(\mu\text{-}sac)]_n$, nano size of $[Pb(H_2O)(\mu\text{-}OAc)(\mu\text{-}sac)]_n$, PbO and PbS). We noticed that the particles size obtained from the BET and the SEM methods, agree very well with the result given by X-ray line broadening. The results of SEM observations and BET methods further confirmed and verified the relevant results obtained by XRD as mentioned above [42–46].

Conclusion

New Pb(II) coordination polymer with saccharine and acetate anions, $[Pb(H_2O)(\mu\text{-}OAc)(\mu\text{-}sac)]_n$, has been synthesized using a thermal gradient approach and a sonochemical method. The compounds are structurally diverse and show interesting three-dimensional coordination polymers. Reduction of the particle size of the coordination polymers to a few dozen nanometers decreases the thermal stability compared to the single crystalline samples. This study demonstrates that the metal–organic framework may be suitable precursors for the preparation of nanoscale materials with interesting morphologies. On this perspective, further systematic studies of other complexes with different metal ions are ongoing in my laboratory, which may offer new insights into metale–organic supramolecular assembly and nanochemistry.

Appendix A. Supplementary material

The crystallographic data (excluding structure factors) for compound has been deposited with the Cambridge Crystallographic Data Centre (CCDC) as supplementary publication number 8 CCDC-857166. Copies of the data can be obtained, free of charge, by application to CCDC, 12 Union Road, Cambridge, CB2 1EZ, UK: (Fax: +44-1223-336033; e-mail: data_request@ccdc.cam.ac.uk), or via the internet: (http://www.ccdc.cam.ac.uk/products/csd/request).

References

[1] S. Leininger, B. Olenyuk, P.J. Stang, Chem. Rev. 100 (2000) 853–907.
[2] S. Karasawa, Y. Sano, T. Akita, N. Koga, T. Itoh, H. Iwamura, P. Rabu, M. Drillon, J. Am. Chem. Soc. 120 (1998) 10080–10087.
[3] D.J. Ager, D.P. Pantaleone, S.A. Henderson, A.L. Katritzky, I. Prakash, D.E. Walters, Angew. Chem. Int. Ed. 37 (1998) 1802.
[4] K.J. Ahmed, A. Habib, S.Z. Haider, K.M.A. Malik, M.B. Hursthouse, Inorg. Chim. Acta 56 (1981) L37.
[5] S.Z. Haider, K.M.A. Malik, K.J. Ahmed, H. Hess, H. Riffel, M.B. Hursthouse, Inorg. Chim. Acta 72 (1983) 21.
[6] S.Z. Haider, K.M.A. Malik, S. Das, M.B. Hursthouse, Acta Crystallogr. 40 (1984) 1147.
[7] G. Jovanovski, B. Kamenar, Cryst. Struct. Commun. 11 (1982) 257.
[8] B. Kamenar, G. Jovanovski, D. Grudenic, Cryst. Struct. Commun. 11 (1982) 241–247.
[9] B. Kamenar, G. Jovanovski, D. Grudenic, Cryst. Struct. Commun. 11 (1982) 257–263.
[10] G. Jovanovski, B. Kamenar, G. Ferguson, B. Kaitner, Acta Crystallogr. 44 (1988) 616.
[11] A. Hergold-Brundic, B. Kamenar, G. Jovanovski, Acta Crystallogr. 45 (1989) 556–561.
[12] F.A. Cotton, G.E. Lewis, C.A. Murillo, W. Schwotzer, G. Valle, Inorg. Chem. 23 (1984) 4038–4041.
[13] V.T. Yilmaz, S. Guney, O. Andac, W.T.A. Harrison, Polyhedron 21 (2002) 2393–2396.
[14] Y. Topcu, O. Andac, V.T. Yilmaz, W.T.A. Harrison, Cryst. Res. Technol. 37 (2002) 509–514.
[15] G.M. Sheldrick, Acta Crystallogr. 46 (1990) 467–472.
[16] A.R. Criswell, R. Bolotovsky, T. Niemeyer, R. Athay, J.W. Pflugrath, Acta Cryst., Section A 60 (2004).
[17] G. M. Sheldrick, C. Kruger, R. Goddard, SHELXS86, Crystallographic Computing 3, Oxford University Press, 175-189.
[18] A.J. Canty, C.L. Raston, B.W. Skelton, A.H. White, Dalton Trans. (1982) 15–20.
[19] I. Persson, M. Sandstrom, P.L. Goggin, A. Mosset, Dalton Trans. (1985), 1597-1560.
[20] S. Hamamci, V.T. Yilmaz, C. Thöne, Acta Crystallogr., Sect. E: Struct. Rep. (Online) 58 (2002) 369–371.
[21] V.T. Yilmaz, S. Hamamci, C. Thöne, Cryst. Res. Technol. 37 (2002) 1143–1148.
[22] S. Hamamci, V.T. Yilmaz, C. Thone, Acta Crystallogr., Sect. E: Struct. Rep. (Online) 58 (12) (2002) 700–701.
[23] V.T. Yilmaz, S. Hamamci, C. Thone, Acta Crystallogr., Sect. E: Struct. Rep. (Online) 58 (12) (2002) 702–704.
[24] M.J. Zaworotko, B. Moulton, Chem. Rev. 101 (2001) 2619.
[25] M. Eddaoudi, D.B. Moler, H. Li, B. Chen, T.M. Reineke, M.O. Keeffe, O.M. Yaghi, Acc. Chem. Res. 34 (2001) 319.
[26] V.T. Yilmaz, S. Hamamci, Ö. Andaç, K. Güven, Z. Anorg. Allg. Chem. 629 (2003) 172–176.
[27] V.T. Yilmaz, S. Hamamci, C. Thone, Z. Anorg. Allg. Chem. 629 (2003) 711–715.

[28] A. Aslani, A. Morsali, Chem. Commun. (2008) 3402–3404.
[29] A. Aslani, A. Morsali, M. Zeller, Dalton Trans. (2008) 5173–5177.
[30] A. Aslani, A. Morsali, Inorg. Chim. Acta 362 (2009) 5012–5016.
[31] A. Aslani, A. Morsali, V.T. Yilmaz, O. Büyükgüngör, Inorg. Chim. Acta 362 (2009) 1506–1510.
[32] A. Aslani, Ali Morsali, V.T. Yilmaz, Canan Kazak, J. Mol. Struct. 929 (2009) 187–192.
[33] Lida Hashemi, A. Aslani, Ali Morsali, J. Inorg. Organomet. Polym. 22 (2012) 1–6.
[34] V. Safarifard, A. Morsali, Ultrason. Sonochem. 19 (2012) 300–306.
[35] M.J.S. Fard, N. Ghanbari, F. Rastaghi, Inorg. Chim. Acta (2013) 149–153.
[36] H. Haddadian, A. Aslani, A. Morsali, Inorg. Chim. Acta 362 (2009) 1805–1809.
[37] F. Marandi, A. Aslani, A. Morsali, J. Coord. Chem. 61 (6) (2008) 882–890.
[38] A. Aslani, A. Morsali, V.T. Yilmaz, C. Kazak, J. Mol. Struct. 929 (2009) 187–192.
[39] A. Aslani, A. Morsali, M. Zeller, Solid State Sci. 10 (2008) 854–858.
[40] A. Aslani, A. Morsali, M. Zeller, Solid State Sci. 10 (2008) 1591–1597.
[41] A. Aslani, A.R.B. Shamili, S. Barzegar, Physica B 405 (2010) 3585–3589.
[42] A. Aslani, A.R.B. Shamili, K. Kaviani, Physica B 405 (2010) 3972–3976.
[43] A. Aslani, Physica B 406 (2011) 150–154.
[44] A. Aslani, V. Oroojpour, Physica B 406 (2011) 144–149.
[45] A. Aslani, M.R. Arefi, A. Babapoor, A. Amiri, K.B. Shuraki, Appl. Surf. Sci. 257 (2011) 4885–4889.
[46] A. Aslani, V. Oroojpour, M. Fallahi, Appl. Surf. Sci. 257 (2011) 4056–4061.